Orphan nuclear receptor estrogen-related receptor α is essential for adaptive thermogenesis

Josep A. Villena*, M. Benjamin Hock*, William Y. Chang†, Joanalyn E. Barcas†, Vincent Giguère‡, and Anastasia Kralli*§

*Department of Cell Biology, The Scripps Research Institute, La Jolla, CA 92037; †Ligand Pharmaceuticals, San Diego, CA 92121; and ‡Molecular Oncology Group, McGill University Health Centre, Montréal, QC, Canada H3A 1A1

Edited by Bert W. O'Malley, Baylor College of Medicine, Houston, TX, and approved November 28, 2006 (received for review September 2, 2006)

Survival of organisms requires the ability to adapt to changes in the environment. Adaptation of oxidative metabolism is essential for meeting increased energy demands in response to stressors, such as exposure to cold temperatures or increased physical activity. Adaptive changes in metabolism are often achieved at the level of gene expression, and nuclear receptors have prevalent roles in mediating such responses. Estrogen-related receptor α (ERRα) was the first orphan nuclear receptor to be identified, and yet its physiologic function remains unknown. Here, we show that mice lacking ERRα are unable to maintain body temperature when exposed to cold. Surprisingly, the inability to adapt to cold is not due to defects in the acute transcriptional induction of genes important for thermogenesis. Rather, we show that ERRα is needed for the high levels of mitochondrial biogenesis and oxidative capacity characteristic of brown adipose tissue (BAT), and thus for providing the energy necessary for thermogenesis. ERRα fulfills this role by acting directly at genes important for mitochondrial function, parallel to other factors controlling mitochondrial gene expression, such as NRF1 and NRF2/GABPA. Our findings demonstrate that ERRα is a key regulator of mitochondrial biogenesis and oxidative metabolism, and essential for adaptive thermogenesis.

mitochondrial biogenesis | oxidative metabolism | brown adipose tissue

Elucidation of the physiologic roles of many nuclear receptor family members has not only revealed their importance in regulating aspects of metabolism but also suggested strategies by which synthetic ligands to such receptors [e.g., peroxisome proliferator-activated receptors (PPARs) or liver X receptor (LXRs)] can impact the treatment of metabolic disease (1). Estrogen-related receptor (ERR) α is an orphan nuclear receptor and the founding member of the small subfamily of Estrogen-Related Receptors, which includes also ERRβ and ERRγ (2–4). Even though progress has been made in identifying cellular pathways regulated by ERRα, the physiologic responses to which ERRα function contributes remain largely unknown (5–8).

ERRα function has been linked to at least three pathways: estrogen signaling, bone formation and oxidative metabolism (reviewed in refs. 4, 9, and 10). Several lines of evidence support an ERRα role in oxidative metabolism. First, ERRα expression is high in tissues with high oxidative capacity (2, 11) and increased at physiologic states of increased energy demand, such as fasting, exposure to cold or exercise (12–14). Second, ERRα activity is regulated by the peroxisome proliferator-activated receptor γ coactivators (PGC)-1α and PGC-1β (13, 15, 16), which coordinate the expression of genes involved in mitochondrial biogenesis and oxidative metabolism (reviewed in refs. 17 and 18). Third, inhibition of ERRα in cultured cells diminishes the ability of PGC-1α to induce mitochondrial biogenesis and cellular respiration (6, 7). Conversely, constitutively active ERRα induces mitochondrial biogenesis and expression of genes with roles in oxidative metabolism (6, 8). Nevertheless, the physiologic role of ERRα *in vivo* is not clear. ERRα-null mice are viable; they show a small decrease in white adipose depots and are resistant to diet-induced obesity, phenotypes that are not consistent with a general decrease in oxidative metabolism (5).

Brown adipose tissue (BAT) is one of the tissues expressing the highest levels of ERRα (19). The function of BAT is to produce heat in response to cold temperatures, via nonshivering adaptive thermogenesis, an energy-dissipating process that is essential for the maintenance of body temperature in small mammals (reviewed in ref. 20). The thermogenic capacity of brown adipocytes relies on their dense mitochondrial reticulum, as well as the BAT-specific expression of thermogenic genes, such as the uncoupling protein 1 (UCP1) (21, 22). Exposure of animals to cold temperatures leads to activation of the sympathetic nervous system and release of norepinephrine, which stimulates BAT cAMP production and induces the thermogenic program: enhanced expression of the coactivator PGC-1α, the uncoupling protein UCP1, and the type 2 iodothyronine deiodinase DIO2, as well as enhanced lipolysis and lipid oxidation. UCP1 uncouples the proton gradient generated by substrate oxidation from ATP synthesis, and thus promotes the generation of heat instead of ATP (21, 22). Failure to properly induce PGC-1α or UCP1 results in defective thermogenesis and the inability to adapt and survive in a cold environment (21, 23, 24).

To gain insights into the physiologic role of ERRα, we determined the consequences of the lack of ERRα on BAT function. We show that mice lacking ERRα are defective in nonshivering adaptive thermogenesis. The impaired thermogenic function is due not to compromised transcriptional induction of the thermogenic program, but to decreased mitochondrial mass and oxidative capacity in brown adipocytes. Our results demonstrate that ERRα is a key component of the tissue-specific transcriptional network that determines high levels of mitochondrial biogenesis and oxidative metabolism in BAT, and essential for survival in situations of high energy demand, such as exposure to cold. These findings also suggest that changes in ERRα activity may contribute to pathophysiological states associated with mitochondrial dysfunction.

Results

Decreased Expression of Mitochondrial Energy Metabolism Genes in ERRα Knockout (KO) Mice. To evaluate the contribution of ERRα to energy metabolism *in vivo*, we compared the mRNA levels of genes with roles in oxidative metabolism in BAT of mice lacking ERRα (ERRα KO) and their WT littermates. Expression of

Author contributions: J.A.V., M.B.H., and A.K. designed research; J.A.V., M.B.H., W.Y.C., and J.E.B. performed research; V.G. contributed new reagents/analytic tools; J.A.V., M.B.H., W.Y.C., J.E.B., and A.K. analyzed data; and J.A.V. and A.K. wrote the paper.

The authors declare no conflict of interest.

This article is a PNAS direct submission.

Abbreviations: ERR, estrogen-related receptor; BAT, brown adipose tissue; NRF, nuclear respiratory factor; GABPA, GA repeat-binding protein α; PGC-1, peroxisome proliferator-activated receptor γ coactivator 1; UCP1, uncoupling protein 1; TCA, tricarboxylic acid cycle; FAO, fatty acid oxidation; OxPhos, oxidative phosphorylation.

§To whom correspondence should be addressed at: Department of Cell Biology, The Scripps Research Institute, 10550 North Torrey Pines Road, La Jolla, CA 92037. E-mail: kralli@scripps.edu.

This article contains supporting information online at www.pnas.org/cgi/content/full/0607696104/DC1.

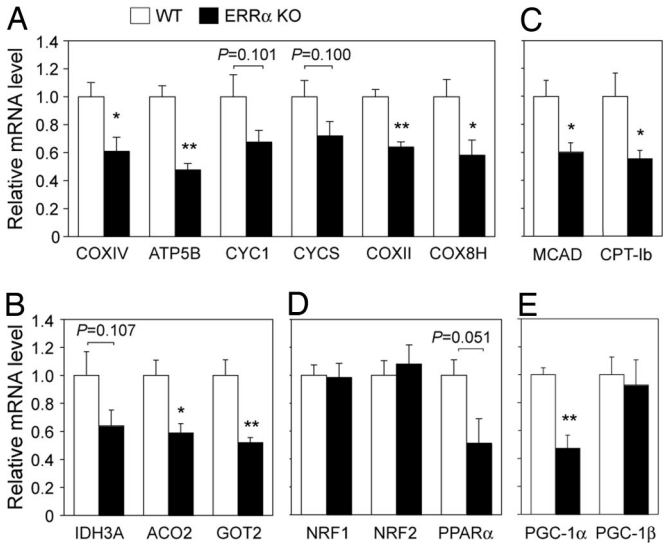

Fig. 1. Decreased expression of mitochondrial energy metabolism genes in BAT of ERRα KO, compared with WT mice. mRNA levels of genes encoding mitochondrial proteins important for OxPhos (*A*), TCA cycle (*B*), and fatty acid oxidation (*C*) in BAT were determined by real-time PCR. Similarly, mRNA levels of transcription factors NRF1, NRF2, and PPARα (*D*) and of coactivators PGC-1α and PGC-1β (*E*) were quantified. Data are expressed relative to levels of each gene in WT BAT (set as equal to 1) and are the mean ± SEM of 5–7 animals per group (10–11 animals for NRF1 and NRF2 quantitation). *, $P < 0.05$; **, $P < 0.01$.

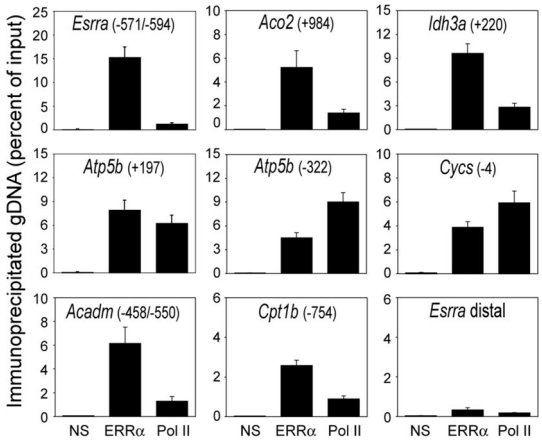

Fig. 2. *In vivo* binding of ERRα to regulatory sequences of mitochondrial genes in BAT. The presence of specific genomic regions in chromatin immunoprecipitated from BAT of WT mice by using antibodies against GFP (control, NS), ERRα, or Pol II was determined by real-time PCR. Numbers in parentheses indicate location of ERRE sequences relative to the transcription start site of each gene (see SI Fig. 9 for sequences). The *Esrra* distal region does not harbor ERREs and was used as a negative control. Data are expressed as percentage of genomic DNA in the immunoprecipitate relative to the input for the same sample and are the mean ± SEM of four mice, processed and assayed independently.

mitochondrial genes important for oxidative phosphorylation (OxPhos), the tricarboxylic acid (TCA) cycle, and fatty acid oxidation (FAO) were decreased by 30–50% in ERRα KO, compared with WT mice (Fig. 1 *A–C*). No differences were observed in the levels of nuclear DNA-binding transcription factors with roles in mitochondrial biogenesis, such as NRF1 or NRF2/GABPA (Fig. 1*D*), suggesting that ERRα regulates BAT mitochondrial gene expression in an NRF-independent manner. Expression of the nuclear receptor PPARα was ≈2-fold decreased (Fig. 1*D*), suggesting that part of the decrease in FAO genes could be by means of effects on PPARα expression (8). Finally, levels of the coactivator PGC-1α were 2-fold reduced in ERRα KO mice, whereas PGC-1β levels were unchanged (Fig. 1*E*). In summary, lack of ERRα led to a decreased expression of genes of the major mitochondrial pathways important for energy production.

***In Vivo* Binding of ERRα to Energy Metabolism Genes in BAT.** To determine whether ERRα acts directly on mitochondrial genes in BAT of mice, we performed ChIP assays with an anti-ERRα antibody and assessed the recruitment of ERRα to target genes. The specificity of the antibody was confirmed by the lack of signal in parallel ChIP assays with BAT of ERRα KO mice [supporting information (SI) Fig. 8], as well as lack of signal in regions lacking ERR response elements (ERREs) (Fig. 2). ERRα in BAT of WT mice was readily detected at the proximal promoter region of its own gene, a region that harbors two tandem ERREs (7, 25) (Fig. 2). ERRα was also present at the regulatory sequences of the TCA cycle genes *Idh3a* and *Aco2*, the OxPhos genes *Atp5b* and *Cycs*, and the FAO genes *Acadm* and *Cpt1b* (Fig. 2; see SI Fig. 9 and refs. 6, 11, and 19 for location and sequence of ERREs). Occupancy of Pol II was also detected at the ERRα targeted genes, consistent with the genes being expressed and the ERREs being close to promoters or in transcribed sequences (first introns). These results demonstrate that ERRα is recruited to promoters of energy metabolism genes *in vivo*, and together with previous studies (6, 15) suggest a direct role for ERRα in the transcriptional regulation of OxPhos, TCA cycle, and FAO genes.

Decreased Mitochondrial Content and Increased Lipid Accumulation in BAT of ERRα KO Mice. We next asked whether the lack of ERRα *in vivo* affects not only expression of energy metabolism genes but also mitochondrial biogenesis, as predicted from cell culture studies (6). Ultra-structural analysis of BAT by transmission electron microscopy showed that brown adipocytes of ERRα KO mice had a lower mitochondrial density, compared with WT (Fig. 3*A*). The cytoplasm of ERRα KO brown adipocytes was readily recognizable in between mitochondria, whereas the cytoplasm of WT adipocytes was filled with tightly packed mitochondria and hardly discernible. Mitochondrial morphology appeared similar in WT and ERRα KO mice. Quantitative measurements indicated 37% fewer mtDNA copies in brown adipocytes of ERRα KO, compared with WT (Fig. 3*B*). Consistent with the decreased mtDNA content, ERRα KO mice had decreased expression of at least four nuclear genes encoding mtDNA transcription/replication factors (SI Fig. 10*A*). Finally, we purified mitochondria from whole BAT and observed a 36% decrease in mitochondrial protein mass in ERRα KO, compared with WT littermates (Fig. 3*C*). These findings demonstrate that ERRα is required for the high mitochondrial content of BAT.

Transmission electron microscopy images of the BAT also revealed that brown adipocytes from ERRα KO mice exhibited a marked increase in intracellular accumulation of triglycerides (Fig. 3*A*). The increase in lipid accumulation was evident during isolation of the tissue, with BAT depots from ERRα KO mice being paler than those of WT and floating in media during isolation, and was confirmed by histological analysis (SI Fig. 11). Measurement of the triglyceride content showed an ≈2.5-fold increase in ERRα KO, compared with WT mice (Fig. 3*D*). Lipid droplets exhibited the typical multivacuolar organization characteristic of brown adipocytes in both WT and ERRα KO mice. However, in ERRα KO mice, triglycerides were distributed in markedly bigger lipid droplets, characteristic of poorly active brown adipocytes (Fig. 3*A* and SI Fig. 11*D*) (26, 27). These findings, together with the decreased expression of FAO genes

PHYSIOLOGY

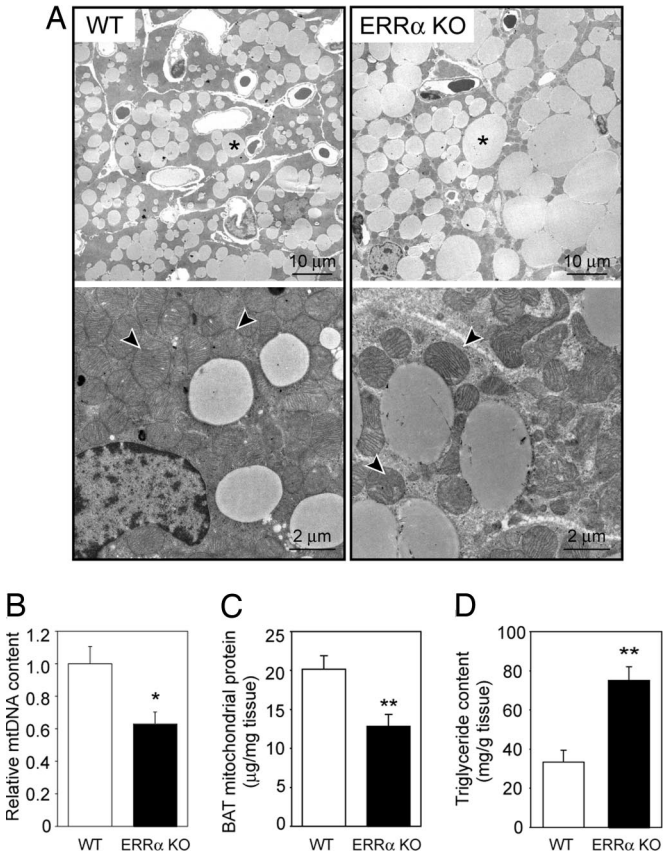

Fig. 3. Decreased mitochondrial mass and increased lipid accumulation in BAT of ERRα KO mice. (*A*) Representative electron microscopy images of BAT of WT (*Left*) and ERRα KO (*Right*) mice; *, triglycerides; arrowheads point to mitochondria. (*B*) mtDNA content in BAT, determined by real-time PCR and expressed relative to content in WT mice. Data are the mean ± SEM of six animals in each group. (*C*) Mitochondrial protein mass in BAT of WT and ERRα KO, measured after purification of mitochondria. Data are expressed as micrograms of mitochondrial protein per milligram of BAT and are the mean ± SEM of four independent experiments with two WT and two ERRα KO mice per experiment. (*D*) Triglyceride content in BAT of WT and ERRα KO mice.

and the decreased mitochondrial content, suggest a defect in the oxidative capacity of ERRα KO BAT.

Impaired Adaptive Thermogenesis in Mice Lacking ERRα. To gain insight into the physiologic significance of the decreased BAT mitochondrial mass in ERRα KO mice, we assessed BAT function by comparing the thermogenic responses of WT and ERRα KO animals. Mice acclimated to thermoneutrality (30°C) were exposed acutely to 4°C for 6 h. Control animals kept at 30°C for the duration of the experiment exhibited a constant body temperature with no differences between WT and ERRα KO mice (WT = 37.3°C ± 0.07, $n = 7$; ERRα KO = 37.4°C ± 0.10, $n = 5$) (Fig. 4*A Left*). When exposed to 4°C, WT mice ($n = 10$) were able to maintain their temperature, exhibiting only a mild decrease (0.42°C) after 6 h. However, ERRα KO mice ($n = 6$) at 4°C failed to maintain their body temperature, which fell an average of 2.3°C in 6 h (Fig. 4*A Right*), suggesting a defect in adaptive thermogenesis.

We next asked whether the inability of ERRα KO mice to maintain body temperature could be due to defects in the transcriptional induction of the thermogenic program. As shown in Fig. 4*B*, UCP1, PGC-1α, and DIO2 mRNA levels were induced to comparable levels in ERRα KO and WT mice (or better in the case of DIO2 in ERRα KO mice), suggesting that

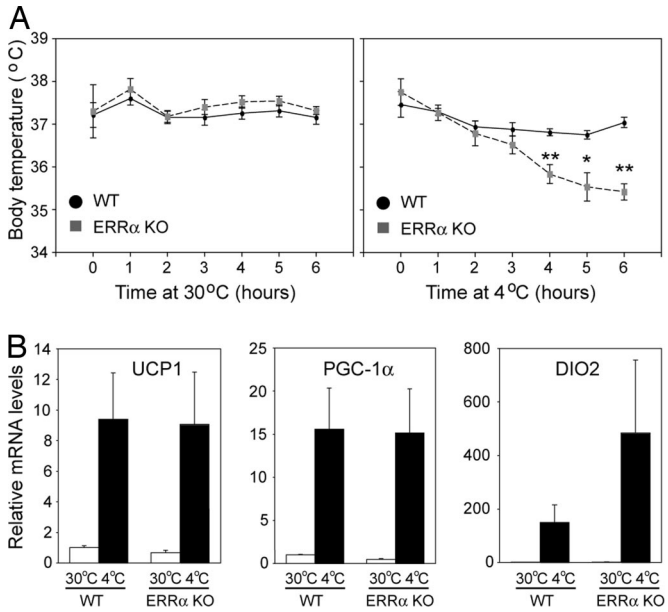

Fig. 4. Impaired thermogenesis in ERRα KO mice upon acute exposure to 4°C. (*A*) Body temperature of WT and ERRα KO mice exposed for 6 h at 30°C (*Left*) or 4°C (*Right*). (*B*) UCP1, PGC-1α, and DIO2 mRNA levels in BAT of WT and ERRα KO mice after 6 h at 30°C or 4°C, determined by real-time PCR. Data are the mean ± SEM of 5–10 animals per group. *, $P < 0.05$; **, $P < 0.01$.

ERRα does not contribute to the acute transcriptional response upon exposure to cold. Because the induction of UCP1 and DIO2 is at least partly under the control of PGC-1α, these findings also show that ERRα does not mediate the effects of PGC-1α on these two "thermogenic" targets.

To investigate the long-term ability of ERRα KO mice to adapt to cold temperatures and to minimize stress associated with manual temperature measurements, we monitored mice at 13°C over several days, using a telemetry system that records continuously body temperature. WT and ERRα KO mice exhibited a similar body temperature when kept at 30°C (WT, 36.43°C ± 0.1, $n = 11$; ERRα KO, 36.81°C ± 0.28, $n = 9$) (Fig. 5 and data not shown). When exposed to 13°C, WT mice kept their body temperature (Fig. 5 *Upper* and data not shown), but a significant number of ERRα KO (5 of 9) progressed to hypothermia within 1–3 days (Fig. 5 *Lower*, and data not shown).

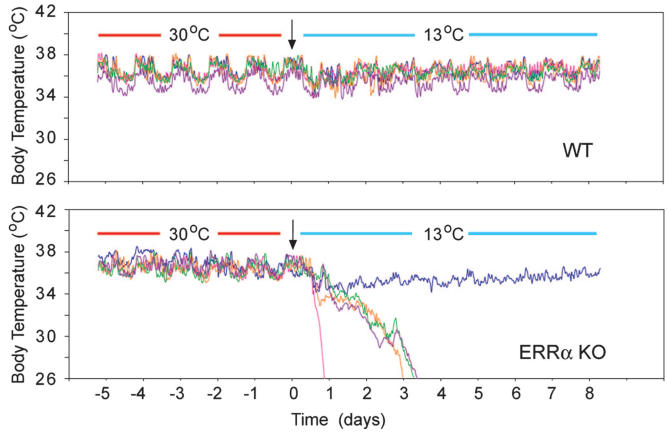

Fig. 5. Impaired thermogenesis in ERRα KO mice during long-term exposure to 13°C. Body temperatures of five WT (*Upper*) and 5 ERRα KO (*Lower*) mice were monitored by telemetry for 5 days at 30°C, followed by 7 days at 13°C. Data shown are from one of two experiments.

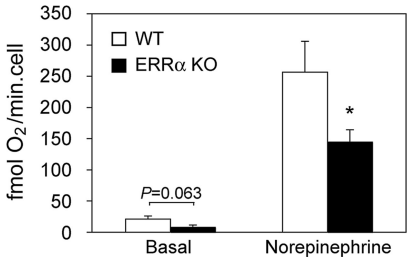

Fig. 6. Decreased respiratory capacity in brown adipocytes isolated from ERRα KO mice. Shown is the respiration of brown adipocytes isolated from WT and ERRα KO mice, measured with a Clark-type oxygen electrode in the absence (basal) or presence of 1 μM norepinephrine. Data are the mean $\pm$ SEM of three independent experiments, with three to six mice and three respiration measurements per experiment. *, $P < 0.05$.

The ERRα KO mice that did not show signs of hypothermia (4 of 9) maintained lower body temperature during the first 24 h of exposure at 13°C (ERRα KO: drop of 3.0°C $\pm$ 1.07, $n = 4$; WT: drop of 0.91°C $\pm$ 0.15, $n = 11$), and recovered their normal body temperature at a slower rate than WT mice (Fig. 5 and data not shown). These data underscore the thermogenic defects observed in ERRα KO mice, which cannot maintain body temperature and whose survival is compromised, even when exposed to moderate low temperatures.

Impaired Respiratory Capacity of Isolated Brown Adipocytes of ERRα KO Mice. Because the thermogenic activity of BAT in response to cold is regulated by the sympathetic nervous system (20) and possible differences in β-adrenergic signaling could contribute to impaired adaptive thermogenesis, we next investigated the oxidative capacity of isolated brown adipocytes *in vitro*, in basal and norepinephrine-stimulated conditions. Basal respiration rates were lower (without reaching statistical significance) in brown adipocytes isolated from ERRα KO than ones from WT littermates (Fig. 6). In the presence of norepinephrine, adipocytes from ERRα KO mice exhibited a significantly impaired respiratory capacity, 56% of that of WT adipocytes (Fig. 6). Notably, ERRα KO brown adipocytes responded as well or even better than WT cells to norepinephrine (17-fold increase in respiratory rates in ERRα KO vs. 12-fold in WT adipocytes). These findings suggest that decreased oxidative capacity is due to intrinsic respiratory defects in ERRα KO adipocytes, rather than defects in β-adrenergic signaling.

Discussion

Energy homeostasis is essential for life. At the transcriptional level, regulation of energy metabolism genes is achieved by a series of DNA binding-factors and cofactors (28, 29). These transcriptional regulators endow cells with not only the basic machinery for energy metabolism, but also tissue-specific components that enable specific physiologic functions and survival in ever-changing environments. We show here that ERRα is an important component of the transcriptional network that achieves high mitochondrial density and high oxidative capacity in BAT. Our findings demonstrate that ERRα regulates mitochondrial biogenesis *in vivo*, as previously suggested by cell culture studies (6). At the physiologic level, ERRα function becomes essential for survival in situations of increased energy demand, such as exposure to cold temperatures. Our findings suggest that decreases in ERRα activity lead to compromised mitochondrial function and reduced capacity for energy production, and ultimately a decline in fitness and survival in situations of metabolic stress.

The primary defect in the BAT of ERRα KO mice is the loss of the tissue-characteristic high mitochondrial density. This loss is reflected in the reduced expression of a wide range of mitochondrial genes (including ones encoding mtDNA transcription/replication factors), reduced mtDNA copy number and protein mass, and decreased cellular oxidative capacity. Importantly, loss of ERRα does not affect brown adipocyte differentiation *per se*. BAT and general adipocyte markers such as UCP1, CIDEA, FABP4, and Col1a1 were maintained properly in ERRα KO mice (Fig. 4; SI Fig. 10). Moreover, the existing mitochondria in ERRα KO BAT are morphologically similar to those in WT BAT, as judged by electron microscopy imaging, and have comparable respiratory capacities when purified and assayed *in vitro* (SI Fig. 12). Taken together, our results suggest that ERRα is essential for the tissue-characteristic adaptation in mitochondrial levels but not for basal mitochondrial biogenesis or the specific respiratory activity of BAT mitochondria.

The decreased mitochondrial content and oxidative capacity in ERRα KO brown adipocytes have significant functional consequences for BAT thermogenic function. Mice lacking ERRα are unable to maintain proper body temperature when exposed acutely to 4°C, and become severely hypothermic even at mild cold temperatures, as seen at 13°C. The inability to maintain body temperature is not due to defects in the thermogenic transcriptional response. PGC-1α, UCP1 and DIO2 mRNAs are induced properly, indicating that ERRα KO mice sense and respond to the cold environment. UCP1 protein levels are also similar in BAT of ERRα KO and WT mice exposed to cold (SI Fig. 13). Moreover, levels of hormones affecting thermogenesis, such as norepinephrine, T4 and glucocorticoids are similar in WT and ERRα KO mice (SI Table 1). Consistent with proper sensing, brown adipocytes of WT and ERRα KO mice respond similarly to adrenergic stimulation *in vitro*. Thus, the defective thermogenesis is likely explained by the reduced cellular capacity for mitochondrial oxidative metabolism, which provides the energy used by UCP1 to generate heat. The impaired thermogenesis of ERRα KO mice is reminiscent of the cold-sensitivity in animals with defects in lipid oxidation (30–32), and underscores the significance of the high BAT mitochondrial content and oxidative capacity for thermogenesis.

Our study unequivocally establishes ERRα as a direct transcriptional regulator of several mitochondrial genes *in vivo*, with ERRα physically present at regulatory sequences of OxPhos, TCA cycle and FAO genes. Many of these genes are also regulated by other transcription factors, such as NRF1, NRF2/GABPA, and PPARα (18, 29). The BAT levels of NRF1 and NRF2/GABPA were not affected by ERRα, indicating that ERRα in BAT acts parallel to, rather than upstream of, NRF1 and NRF2/GABPA (Fig. 7). In contrast, PPARα expression in BAT was decreased, consistent with previous studies (8) and a role of ERRα both upstream and parallel to PPARα (Fig. 7). Notably, the phenotype of ERRα KO mice differs from that of PPARα KO mice, which show decreased body temperature in response to fasting but not in response to cold (33). Thus, it seems likely that ERRα and PPARα regulate overlapping sets of genes, possibly in response to different signals, and have distinct physiologic functions in BAT.

ERRα acts as a downstream effector of PGC-1α in the regulation of many energy metabolism genes (6–8, 34). Interestingly, our findings show that ERRα does not merely mediate all PGC-1α functions in BAT. In particular, ERRα is not required for the acute transcriptional response to cold. Rather, ERRα acts on a subset of PGC-1α-regulated genes, affecting predominantly lipid oxidation, enzymes of the TCA cycle, OxPhos components and the cellular mitochondrial content (Fig. 7). Notably, the defects in this ERRα-defined set of targets seem more pronounced in the ERRα KO mice than PGC-1α KO mice, which do not show a significant decrease in BAT mitochondrial content (23, 24). The more severe defect in ERRα KO animals is likely explained by ERRα acting downstream of other coregu-

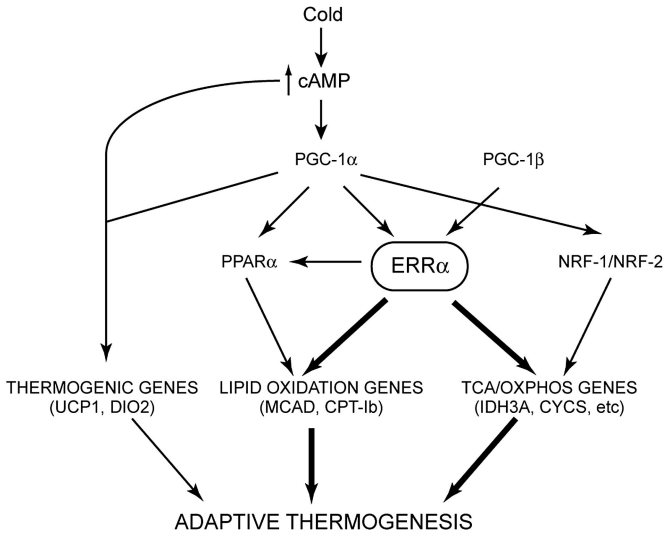

Fig. 7. Proposed role of ERRα in the BAT pathways required for adaptive thermogenesis.

lators, besides PGC-1α. For example, ERRα activity is regulated by the coactivator PGC-1β, which also drives BAT mitochondrial biogenesis (16, 35).

ERRα is expressed in other tissues with high oxidative capacity, besides BAT (2, 11). Decreased expression of energy metabolism genes is also seen in intestine, liver, muscle and CNS of ERRα KO mice (refs. 36 and 37 and data not shown), indicating similar functions of ERRα in these tissues. Nevertheless, ERRα KO mice do not show reduced energy expenditure and are resistant to diet-induced obesity (5). This seemingly paradoxical phenotype may be due to the up-regulation of parallel compensatory pathways in a tissue-specific manner. PGC-1α expression is increased in heart, liver and muscle of ERRα KO mice, ERRγ expression is increased in heart and WAT, and PPARα in WAT (refs. 8 and 37 and data not shown). Consistent with the increased levels of these transcriptional regulators, expression of the thermogenic and energy expenditure promoting gene UCP1 is increased in the inguinal WAT depot of ERRα KO (ref. 5 and data not shown). In summary, changes in the expression of energy metabolism genes in ERRα KO mice are consistent with decreased oxidative metabolism and energy expending capacity in some tissues, such as BAT, and increased energy expenditure in other tissues, such as inguinal WAT.

In conclusion, the studies presented here show that ERRα is an important component of the regulatory network that controls mitochondrial biogenesis and function *in vivo*. The decrease in BAT mitochondrial mass and oxidative function in the ERRα KO mice reduces organism fitness in cold environments. Notably, ERRα KO mice have reduced fitness even in standard housing conditions, with only 76% of ERRα homozygous null mice reaching weaning age. The physiologic consequences of ERRα lack of function in tissues other than BAT is currently unclear. Further studies will be required to assess how lack of ERRα affects other situations of increased metabolic demand where ERRα has been implicated, e.g., the adaptation to physical exercise in muscle (14).

Materials and Methods

Animals. Generation of ERRα-null mice (ERRα KO) and their backcross into the C57BL/6 genetic background have been described (5). Mice were housed at 22°C on a 12-h light–dark cycle with free access to food (standard chow diet LM-485; Harland Tekland, Indianapolis, IN) and water. Procedures involving animals were approved by the Institutional Animal Care and Use Committee of The Scripps Research Institute.

Gene Expression. RNA was isolated from interscapular BAT by using TRIzol (Invitrogen, Carlsbad, CA), according to the manufacturer's instructions. cDNA was synthesized from 400 ng of RNA with SuperScript II reverse transcriptase (Invitrogen) and oligo(dT) primers. Gene expression was assessed by quantitative PCR by using gene-specific primers (see SI Table 2) and SYBR green (Applied Biosystems, Foster City, CA) in a PTC-200 thermal cycler (Bio-Rad, Hercules, CA) coupled to a Chromo4 real-time PCR detection system (Bio-Rad). mRNA expression data were normalized by using cyclophilin A as a reference gene.

ChIP. Interscapular BAT from 4-month-old WT mice was dissected, minced, passed 25 times through an 18-gauge needle, and incubated for 20 min at room temperature in 1 ml of PBS containing 1% formaldehyde. Cross-linking was arrested by addition of glycine (final concentration 125 mM). Tissue was then washed in PBS, resuspended in 500 μl of buffer (25 mM Tris, pH 8.0/2 mM EDTA/150 mM NaCl/1% Triton X-100/0.1% SDS), sonicated, and centrifuged at 11,000 $\times$ *g* for 20 min. Soluble chromatin was precleared by incubation with protein A-/protein G-Sepharose for 2 h at 4°C, and incubated overnight at 4°C with control [anti-GFP; Roche Molecular Biochemicals (Indianapolis, IN) no. 1814460], anti-ERRα (19), or anti-Pol II (sc-899; Santa Cruz Biotechnology, Santa Cruz, CA) antibodies. After an additional incubation with protein A-/protein G-Sepharose for 2 h at 4°C, immunocomplexes were processed as described (14). Input and immunoprecipitated samples were analyzed by using real-time PCR and gene-specific primers (SI Table 2) to determine the copy number of specific DNA regions. Data were expressed as percent of genomic DNA immunoprecipitated, i.e., amount in immunoprecipitate relative to input sample.

Thermogenic Response to Cold Exposure. For the acute cold exposure, 10- to 13-week-old WT and ERRα KO male littermates that had been acclimated to thermoneutrality (30°C) for 10 days were transferred to 4°C for 6 h with full access to water and food. Control WT and ERRα KO animals remained at 30°C. Body temperature was measured every hour by using a digital thermometer with a colonic probe. At 6 h, control and cold-exposed mice were euthanized, and the interscapular BAT was isolated.

For the long-term exposure at 13°C, 9- to 12-week-old WT and ERRα KO male littermates were first acclimated at thermoneutrality for 15 days and then switched to 13°C for 7 days. Body temperatures and activity were recorded during the last 5 days of the acclimation period at 30°C and for the 7 days at 13°C by telemetry, by using an RPC-1 receiver and the Dataquest acquisition system (Data Science International, St. Paul, MN). At the end of the 7-day period, animals were euthanized, and their BAT was dissected for analysis. Animals whose body temperature dropped below 26°C during the course of the experiment were removed early and euthanized.

Morphological Analysis of BAT. For histological analysis, interscapular BAT was dissected clean from white adipose tissue and muscle, washed in PBS, fixed overnight in 10% formalin, dehydrated, and embedded in paraffin for sectioning. Eight- to 10-μm sections were stained with hematoxylin/eosin.

For transmission electron microscopy, interscapular BAT was dissected as described above, cut into small pieces ($\approx$1 mm^2), and fixed overnight with 2.5% glutaraldehyde/2% paraformaldehyde in 0.1 M phosphate buffer (pH 7.4). Samples were then washed in 0.1 M sodium cacodylate buffer and postfixed for 5 h with 1% OsO_4 in cacodylate buffer. Samples were dehydrated in a graded

ethanol series and embedded in Epon/Araldite resin overnight. Ultrathin sections were obtained, contrasted with uranyl acetate/lead citrate, and examined with a Philips CM100 microscope.

BAT Triglyceride Content. Total lipids from BAT were extracted in a mixture of 2:1 chloroform/methanol and washed once with 0.2 vol of 0.9% NaCl. Triglycerides were measured by using Infinity Triglyceride reagent (Sigma, St. Louis, MO).

Mitochondrial DNA Quantification. Total DNA was isolated from BAT of 10- to 13-week-old mice and treated with RNase A. The mtDNA content relative to nuclear DNA was assessed by quantitative PCR by using 2 ng of total DNA as template and primers (SI Table 2) for COXII (mitochondrial genome) and RIP140 (nuclear genome).

Mitochondrial Protein Quantification. Interscapular, axillar, and cervical BAT depots were pooled, homogenized by using a Potter-Elvehjem tissue homogenizer in buffer H (0.25 M sucrose/5 mM TES/0.2 mM EGTA/0.5% fatty acid-free BSA, pH 7.2), and centrifuged at 8,500 $\times$ *g* for 10 min. The mitochondria-containing pellet was resuspended in buffer H and centrifuged at 800 $\times$ *g* for 10 min. Next, the supernatant was centrifuged at 8,500 $\times$ *g* for 10 min to recover the mitochondrial fraction. The pelleted mitochondria were washed once and resuspended in KCl/TES buffer (100 mM KCl/20 mM TES, pH 7.2). Protein content was measured by using the Bradford method (Pierce, Rockford, IL).

Respiration in Isolated Brown Adipocytes. Pooled interscapular, cervical, and axillar BAT depots from two to six mice in each experiment were washed in PBS, minced with scissors, and digested with collagenase for 30–40 min at 37°C with constant shaking in digestion buffer (100 mM Hepes, pH 7.4/123 mM NaCl/5 mM KCl/1.3 mM $CaCl_2$/5 mM glucose/1.5% BSA/1 mg/ml Collagenase A), vortexing the samples every 10 min. The digested tissue was filtered through a 70-μm nylon cell strainer, and the cell suspension was centrifuged at 65 $\times$ *g* for 5 min. The upper phase containing floating adipocytes was washed with DMEM:F12 cell culture media and centrifuged at 65 $\times$ *g* for 5 min. After discarding infranatant, brown adipocytes were resuspended in DMEM:F12 media, counted, and immediately used for respiration measurements.

Oxygen consumption was monitored with a Clark-type oxygen electrode (Hansatech Instruments Ltd, Norfolk, U.K.), by using 4.5–6 $\times$ 10^4 freshly isolated brown adipocytes in respiration media (DMEM: F12/5% CO_2, pH 7.4) and with constant agitation. Basal respiration was measured for 2–3 min, after which 1 μM norepinephrine was added and oxygen consumption was monitored for 3–5 min. Maximal respiration rates were calculated as the average rate over a 1-min period, after subtracting background. Background was estimated as the oxygen decrease measured over 1 min after inhibition of mitochondrial respiration by 1 mM KCN.

Hormone Measurements. See *SI Materials and Methods*.

Statistical Analysis. Data are expressed as mean $\pm$ SEM. The statistical significance of differences between samples was determined by a two-tailed Student *t* test.

We thank J. Cardenas and F. Jamarillo for technical assistance; M. Wood and the microscopy core facility at The Scripps Research Institute for the EM studies; T. Earley and A. Patapoutian for assistance with the telemetry system; T. Gettys (Pennington Biomedical Research Center, Baton Rouge, LA) for the UCP1 antibody; and C. Kohler, I. Scheffler, J. Miner, and U. Mueller for advice and discussions. This work was supported by National Institutes of Health Grants DK064951 and DK074660 (to A.K.) and by the Canadian Institutes for Health Research (V.G.).

1. Glass CK (2006) *J Clin Invest* 116:556–560.
2. Giguère V, Yang N, Segui P, Evans RM (1988) *Nature* 331:91–94.
3. Eudy JD, Yao S, Weston MD, Ma-Edmonds M, Talmadge CB, Cheng JJ, Kimberling WJ, Sumegi J (1998) *Genomics* 50:382–384.
4. Giguère V (2002) *Trends Endocrinol Metab* 13:220–225.
5. Luo J, Sladek R, Carrier J, Bader JA, Richard D, Giguère V (2003) *Mol Cell Biol* 23:7947–7956.
6. Schreiber SN, Emter R, Hock MB, Knutti D, Cardenas J, Podvinec M, Oakeley EJ, Kralli A (2004) *Proc Natl Acad Sci USA* 101:6472–6477.
7. Mootha VK, Handschin C, Arlow D, Xie X, St. Pierre J, Sihag S, Yang W, Altshuler D, Puigserver P, Patterson N, *et al*. (2004) *Proc Natl Acad Sci USA* 101:6570–6575.
8. Huss JM, Torra IP, Staels B, Giguère V, Kelly DP (2004) *Mol Cell Biol* 24:9079–9091.
9. Horard B, Vanacker JM (2003) *J Mol Endocrinol* 31:349–357.
10. Bonnelye E, Aubin JE (2005) *J Clin Endocrinol Metab* 90:3115–3121.
11. Vega RB, Kelly DP (1997) *J Biol Chem* 272:31693–31699.
12. Ichida M, Nemoto S, Finkel T (2002) *J Biol Chem* 277:50991–50995.
13. Schreiber SN, Knutti D, Brogli K, Uhlmann T, Kralli A (2003) *J Biol Chem* 278:9013–9018.
14. Cartoni R, Leger B, Hock MB, Praz M, Crettenand A, Pich S, Ziltener JL, Luthi F, Deriaz O, Zorzano A, *et al*. (2005) *J Physiol (London)* 567:349–358.
15. Huss JM, Kopp RP, Kelly DP (2002) *J Biol Chem* 277:40265–40274.
16. Kamei Y, Ohizumi H, Fujitani Y, Nemoto T, Tanaka T, Takahashi N, Kawada T, Miyoshi M, Ezaki O, Kakizuka A (2003) *Proc Natl Acad Sci USA* 100:12378–12383.
17. Lin J, Handschin C, Spiegelman BM (2005) *Cell Metab* 1:361–370.
18. Finck BN, Kelly DP (2006) *J Clin Invest* 116:615–622.
19. Sladek R, Bader JA, Giguère V (1997) *Mol Cell Biol* 17:5400–5409.
20. Cannon B, Nedergaard J (2004) *Physiol Rev* 84:277–359.
21. Enerback S, Jacobsson A, Simpson EM, Guerra C, Yamashita H, Harper ME, Kozak LP (1997) *Nature* 387:90–94.
22. Matthias A, Ohlson KB, Fredriksson JM, Jacobsson A, Nedergaard J, Cannon B (2000) *J Biol Chem* 275:25073–25081.
23. Lin J, Wu PH, Tarr PT, Lindenberg KS, St. Pierre J, Zhang CY, Mootha VK, Jager S, Vianna CR, Reznick RM, *et al*. (2004) *Cell* 119:121–135.
24. Leone TC, Lehman JJ, Finck BN, Schaeffer PJ, Wende AR, Boudina S, Courtois M, Wozniak DF, Sambandam N, Bernal-Mizrachi C, *et al*. (2005) *PLoS Biol* 3:e101.
25. Laganiere J, Tremblay GB, Dufour CR, Giroux S, Rousseau F, Giguère V (2004) *J Biol Chem* 279:18504–18510.
26. Jimenez M, Leger B, Canola K, Lehr L, Arboit P, Seydoux J, Russell AP, Giacobino JP, Muzzin P, Preitner F (2002) *FEBS Lett* 530:37–40.
27. de Jesus LA, Carvalho SD, Ribeiro MO, Schneider M, Kim SW, Harney JW, Larsen PR, Bianco AC (2001) *J Clin Invest* 108:1379–1385.
28. Picard F, Gehin M, Annicotte J, Rocchi S, Champy MF, O'Malley BW, Chambon P, Auwerx J (2002) *Cell* 111:931–941.
29. Kelly DP, Scarpulla RC (2004) *Genes Dev* 18:357–368.
30. Guerra C, Koza RA, Walsh K, Kurtz DM, Wood PA, Kozak LP (1998) *J Clin Invest* 102:1724–1731.
31. Tolwani RJ, Hamm DA, Tian L, Sharer JD, Vockley J, Rinaldo P, Matern D, Schoeb TR, Wood PA (2005) *PLoS Genet* 1:e23.
32. Exil VJ, Gardner CD, Rottman JN, Sims H, Bartelds B, Khuchua Z, Sindhal R, Ni G, Strauss AW (2006) *Am J Physiol* 290:H1289–H1297.
33. Kersten S, Seydoux J, Peters JM, Gonzalez FJ, Desvergne B, Wahli W (1999) *J Clin Invest* 103:1489–1498.
34. Willy PJ, Murray IR, Qian J, Busch BB, Stevens WC, Jr, Martin R, Mohan R, Zhou S, Ordentlich P, Wei P, *et al*. (2004) *Proc Natl Acad Sci USA* 101:8912–8917.
35. Uldry M, Yang W, St. Pierre J, Lin J, Seale P, Spiegelman BM (2006) *Cell Metab* 3:333–341.
36. Carrier JC, Deblois G, Champigny C, Levy E, Giguère V (2004) *J Biol Chem* 279:52052–52058.
37. Herzog B, Cardenas J, Hall RK, Villena JA, Budge PJ, Giguère V, Granner DK, Kralli A (2006) *J Biol Chem* 281:99–106.